Journal of Hazardous Materials 341 (2018) 93–101

Contents lists available at ScienceDirect

Journal of Hazardous Materials

journal homepage: www.elsevier.com/locate/jhazmat

Photoexcitation effect on the adsorption of hazardous gases on silica surface

Yonggang Yang[a], Donglin Li[a], Chaozheng Li[a], Yufang Liu[a,*], Kai Jiang[b]

[a] College of Physics and Materials Science, Henan Normal University, Xinxiang 453007, China
[b] School of Environment, Henan Normal University, Xinxiang 453007, China

HIGHLIGHTS

- A sample of photoexcitation effect on adsorption of adsorbent is proposed.
- Adsorption relies not on hydrogen bond but charge transfer after photoexcitaion.
- Photoexcitation effect is presented as a new standard for detection of adsorbent.

ARTICLE INFO

Article history:
Received 26 February 2017
Received in revised form 11 July 2017
Accepted 24 July 2017
Available online 25 July 2017

Keywords:
Photoexcitation effect
Adsorption
Hazardous gas
Hydrogen bond
Silica surface

ABSTRACT

There is very little scientific understanding of photoexcitation effect on the adsorption properties of adsorbent. The adsorption of four hazardous gases (SARIN (propan-2-ylmethylphospho-nofluoridate), methyl dichlorophosphate (MDCP), trimethyl phosphate (TMP) and hydrogen sulfide (H_2S)) on silica surface is taken as target sample in this work. The adsorption energy order (MDCP < SARIN < TMP) in the ground state is consistent with the strength order of intermolecular hydrogen bond (inter-HB) between hydroxyl group of silica surface and hazardous gas, and the desorption order of the three gases in previous reports. However, with the adsorption energy increase of MDCP and the decrease of SARIN and TMP, this order changes remarkably to SARIN < TMP < MDCP after photoexcitation to excited state by absorbing shortwave ultraviolet irradiation. This change is opposite to the inter-HB weakening of MDCP in the first excited (S_1) state and the strengthening of TMP and SARIN in the second excited (S_2) state. This opposite change is caused by formation of intermolecular charge transfer state of MDCP and local excitation of SARIN and TMP. The H_2S is dissociated after photoexcitation to the S_1 state. This work presents photoexcitation as a new standard for the design and detection of adsorption properties of adsorbent for its striking effect on adsorption behaviors.

1. Introduction

Many technologies have been developed to detect chemical warfare agents (CWAs) and decompose them into nontoxic substances, because of their severe environment contamination and highly deleterious effects on humans [1–4]. Among these CWAs, the nerve agents, such as SARIN and soman, have attracted much concern due to high lethality and have become one of the greatest threats in modern world for the possible use in warfare or terrorist attacks [1,3,5,6]. Surface chemistry of CWAs simulants on environmental materials has become a demanding scientific problem, and is also critical to the rational design of adsorbents and decontamination strategies [1,7–11]. Researchers have designed many simulants of target nerve agents without extreme toxicity, which cannot fully mimic real environmental fate [9,10]. Theoretical approach can eliminate nerves agents' hazards and bring fundamental insight into wide range of conditions, and thus has become a forceful tool for investigating nerves agents-environmental surface interaction [10].

As one of the most abundant materials in environment, the amorphous silica has been utilized as excellent surrogate and test system for exploring nerve agent gas-surface intermolecular interactions [1,8,12–17]. It has been widely used as adsorbent and catalyst support for its relatively high surface area and unique surface properties [18]. The hydroxylation of silica surface is of critical importance and major concern in the design of a decontamination system because of its controllability [1,11,19–27]. Adsorption of gas-phase molecules to silica surface has been the subject of research in many branches of science [19–28]. The adsorption of silica is known to depend largely on the surface hydroxyl (silanol)

* Corresponding author.
E-mail address: liuyufang2005@126.com (Y. Liu).

http://dx.doi.org/10.1016/j.jhazmat.2017.07.052
0304-3894/

groups by forming strong hydrogen bonds primarily between surface silanol groups and the oxygen atom of the P═O moiety in the adsorbate [12,28,29].

Many researches have been conducted to better understand the adsorption of nerve agents to silica and design more effective sensing methods [27,30]. Organophosphorous (OP) compounds mimic the structure and surface chemistry of nerve agents with low toxicity [28]. Wilmsmeyer and coworkers have demonstrated that the simulants (methyl dichlorophosphate (MDCP), dimethyl cholor-ophosphate (DMCP), trimethyl phosphate (TMP), dimethyl methylphosphonate (DMMP) and diisopropyl methylphosphonate (DIMP)) are adsorbed on silica surface through intermolecular hydrogen bond between P═O group and the surface hydroxyl, which is confirmed by their infrared spectroscopy [12,23,31,32]. The strength order of the adsorption follows the trend MDCP < DMCP < TMP < DMMP < DIMP. MDCP, DMMP and TMP are desorbed from silica at 150 °C, 300 °C and at 400 °C respectively [12,23,31]. Temperature is an important factor in affecting adsorption properties of these organophosphorous gases to silica [33]. Moreover, it is demonstrated that the adsorption of DMMP on silica surface depends largely on the hydroxyl coverage of the silica surface [1].

Besides temperature and hydroxyl coverage, photoexcitation effect on the adsorption behaviors of adsorbent has not been extensively studied to our best knowledge. Under normal conditions, silica and its adsorbed complexes are located at ground state, which indicates the lowest energy state and the zero-point energy of the system [34–36]. The ground state of these molecular systems tends to be stable unless the molecular system absorbs energy which is equal to the difference between the ground state and higher state (called excited state). The excited state is a quantum state of the system with higher energy than the ground state [36,37]. These excitation energies are often obtained from irradiation of different wave band, laser, heat and other energy sources. This transition progress occurs with the molecular orbital transition, charge distribution and geometric change, which will induce different changes of adsorption/desorption behaviors. In this work, photoexcitation effect on the adsorption behaviors of four hazardous gases on silica surface will be discussed in detail.

Adsorbent will be excited to the first excited (S_1) state or higher state (Sn, $n \geq 2$) after absorbing transition energy from ultraviolet (UV) light or other energy sources, which will induce different adsorption behaviors, such as adsorption strengthening, desorption or dissociation. Adsorption in the ground state plays a crucial role in the adsorption strength for the adsorbent with large transition energy. The analysis of transition energy and photoexcitation effect will become an important environment effect on adsorption properties of adsorbent. Many works have been reported on study the adsorption of mimetic organophosphonates to silica in the ground state [9–12,22–24,8,31,38–41]. In this work, the adsorption of four hazardous gases to silica before and after photoexcitation is provided as target sample. Samples of nerve agents' simulants (MDCP, TMP), SARIN and hydrogen sulfide are chosen to study their adsorption properties and dynamics behaviors on silica surface in the ground state and excited state. Hydrogen sulfide (H_2S), a toxic gas in the industrial gases, can cause irritation to human health and acidic rains [41–43]. This study will take photoexcitation effect as a new standard for the design and detection of adsorption properties of adsorbent, which will provide comprehensive explanation on adsorption behaviors together with temperature and other environment effects.

2. Theoretical methods

The geometric structures, electronic and infrared spectra of the four complexes are calculated using Gaussian 09 program suite [44]. Becke's three-parameter hybrid exchange function with Lee-Yang-Parr gradient-corrected correlation functional (B3-LYP functional), in combination with 6–31G* basis set, is used in both the Density functional theoretical (DFT) and TDDFT methods [45,46]. The entire local minimums are confirmed by the absence of any imaginary frequency in vibrational analysis calculations. The wave function analysis is performed by the Multiwfn program in order to obtain the information about reduced density gradient (RDG), electrostatic potential value, electron-hole, the bonding energy, and the Lorentz oscillator [47].

3. Results and discussion

The adsorption of organophosphorous compounds (MDCP, SARIN, TMP) and hydrogen sulfide to silica surface is governed by the intermolecular hydrogen bond interaction. Excited state hydrogen bonding dynamics have been demonstrated to be a reliable tool for studying intermolecular interaction and their dynamic behaviors [48–53]. For convenience, hydrogen bonded complexes for MDCP, SARIN, TMP and H_2S with silica suface are denoted as their monomers. In this work, the adsorption change of MDCP, SARIN, TMP and H_2S on silica surface in excited state are investigated by focusing on the adsorption energy change and dynamics behaviors of intermolecular hydrogen bonding before and after photoexcitation.

3.1. Optimized geometric structures in the ground state and the excited state

The bond lengths and angles of the four complexes in ground and excited states are denoted in For MDCP in Fig. 1A and B, the bond length of P═O···H—O is calculated to be 1.813 Å in the ground state, which lengthens to 1.855 Å after photoexcitation to the excited S_1 state. The bond lengths of P═O and O—H, which are involved in the formation of P═O···H—O, respectively lengthen about 0.105 Å and shorten about 0.002 Å in the S_1 state. The angle OHO changes little from ground state (163°) to the S_1 state (165°), implying a slight change in hydrogen bond interaction sites of P═O···H—O. These changes indicate that the intermolecular hydrogen bond P═O···H—O is weakened when excited to the S_1 state, indicating that the adsorption strength of MDCP on silica surface is weakened compared to that in the ground state. We focus on the second excited (S_2) states of SARIN and TMP because of their small transition probability in the S_1 states. For SARIN in Fig. 1C and D, the bond length of P═O···H—O decreases from 1.741 Å in the ground state to 1.477 Å in the excited S_2 state. The bong length change of P═O···H—O of TMP is similar to that of SARIN, decreasing from 1.716 Å in the ground state to 1.477 Å in the S_2 state. The changes of SARIN and TMP indicate that the intermolecular hydrogen bonds are both strengthened compared to the ground state, implying that the adsorption of SARIN and TMP are both strengthened in the S_2 state compared to ground state. The bond lengths of intermolecular hydrogen bonds of MDCP, SARIN and TMP are consistent with the theoretical results obtained by Troya [28]. In Fig. 1G and H, the silica with two silanol groups is hydrogen bonded with hydrogen sulfide by two O—H···S intermolecular hydrogen bonds, denoted as O_1—H_1···S and O_2—H_2···S. It is observed that the bond lengths of O_1—H_1···S and O_2—H_2···S are 2.602 Å and 2.574 Å respectively, which change to 2.580 Å and 2.603 Å when excited to the S_2 state. This change indicates that intermolecular hydrogen bond O_1—H_1···S is strengthened and O_2—H_2···S is weakened in the S_2 state compared to that in the ground state. The angle O_1H_1S changes little, while the angle O_2H_2S decreases largely from 166° in the ground state to 79° in the excited S_2 state. It is interesting to observe that one of the S-H bonds is cleaved in the S_2 state, indicating dissociation of H_2S after photoexcitation. The bond length and

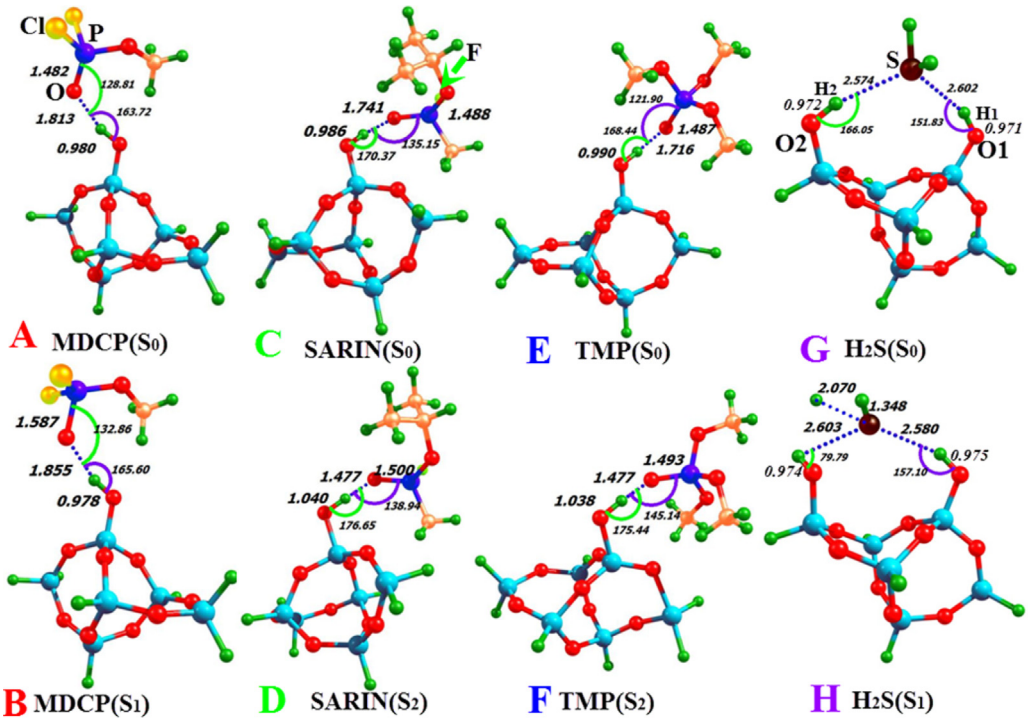

Fig. 1. The calculated bond length and angles of MDCP, SARIN, TMP and H_2S in ground and excited states.

angle of these four complexes after photoexcitation change in different ways, providing evidence for the adsorption change of the three organophosphorous compounds and hydrogen sulfide. The reason for these changes will be discussed in detail in the following section.

3.2. Excitation energy and adsorption energy analysis

The calculated electronic excitation energies (nm) and corresponding oscillator strengths (f), and three indicators (Δr, S and T) of MDCP, SARIN, TMP and H_2S are shown in Table 1. It is reported by Gasparro that ultraviolet radiation is composed of wavelengths between 100 and 400 nm that are further divided into UVC (100–290 nm), UVB (290–320 nm) and UVA (320–400 nm) [54]. The destruction of ozone apparently leads to an increase in shortwave-ultraviolet (UV) on earth because ozone can efficiently absorb UV radiation with wavelength shorter than 300 nm, in particular UVC (below 280 nm), and UV-B (in a specific range of 280–300 nm) [55,56]. By absorbing UVC irradiation, the four complexes can be photoexcited to excited states.

The S_1 state of MDCP has large oscillator strength than that of S_2 state and has excitation energy about 203 nm. For SARIN and TMP, the electronic excitation energies and corresponding oscillator strengths of the S_1 and S_2 states are similar to each other, and the S_2 state has larger oscillator strength than that of S_1 state. Therefore, the S_2 states of SARIN and TMP are discussed in this work. Three indicators (Δr, S and T) are provided to check whether the excited states of four complexes are local excited (LE) or charge transfer (CT) states. The Δr index is proposed as a quantitative indicator of electron excitation mode [57]. The smaller the Δr index is, the more likely the excitation belongs to a LE state. The index S is integral of overlap of hole-electron, and D denotes the distance between centroid of hole and electron. The S_1 state of MDCP has small S and large D/Δr, which indicates that the two excited states of MDCP are charge transfer (CT) state. The S_2 state of SARIN has larger S, smaller D and Δr, indicating that the S_2 state of MDCP is local excited (LE) state. The S_2 state of TMP is similar to that of SARIN and the S_1 state of H_2S is a LE state. The analysis of electronic transition energy can provide evidence for high or low transition energy with corresponding transition probability, and then decide which state to be studied.

The adsorption energies of MDCP, SARIN and TMP are calculated to be −40.678 kJ/mol, −54.283 kJ/mol and −57.831 kJ/mol respectively in the ground state. These adsorption energies follow the order MDCP < SARIN < TMP, which is consistent with the strengthening of intermolecular hydrogen bond interaction and desorption order of MDCP and TMP in previous related reports [28]. This order implies that intermolecular hydrogen bond is the major contribution to the adsorption strength. The adsorption energy of MDCP increases to −53.433 kJ/mol when excited to the S_1 state, while that of SARIN and TMP respectively decreases to −9.207 kJ/mol and −10.566 kJ/mol in the S_2 states. The intermolecular hydrogen bond of MDCP is weakened while that of SARIN and TMP is strengthened. It should be noted that the adsorption energy change of the three complexes is opposite to the change of intermolecular hydrogen bonds in excited state, implying that adsorption behaviors in excited state are remarkably different from those in the ground state and that intermolecular hydrogen bond may not be the major contribution to the adsorption strength. The adsorption energy of H_2S changes to 56.783 kJ/mol in the S_1 state from −27.464 kJ/mol in the ground state, implying desorption of H_2S in the S_1 state. This change is consistent with the dissociation of H_2S in geometric structure analysis.

3.3. Reduced density gradient (RDG) analysis

Johnson et al. have developed an approach to detect noncovalent interactions in real space based on the electron density and its derivatives [58]. The wave functions were analyzed by the Multiwfn program for information on RDG [47]. Fig. 2 shows the gradient isosurfaces and related plots of the reduced density gradient versus the electron density multiplied by the sign of the second Hessian eigenvalues. The gradient isosurfaces are colored according to the corresponding values of sign(λ_2)ρ, which is found to be a good indi-

Table 1
Excitation energy (nm) and corresponding oscillator strengths of MDCP, SARIN, TMP and H_2S in the S_1 and S_2 states. The symbol f denotes oscillator strength, S is integral of overlap of hole-electron, D denotes the distance between centroid of hole and electron, Δr denotes quantitative indicator of electron excitation mode. ΔE denotes the adsorption energy (kJ/mol).

	MDCP		SARIN		TMP		H_2S	
	S_1 203	S_2 201	S_1 157	S_2 154	S_1 154	S_2 152	S_1 196	S_2 168
f	0.0032	0.0000	0.0003	0.0037	0.0002	0.0042	0.0002	0.0003
S	0.141	0.006	0.200	0.225	0.189	0.210	0.239	0.021
D	3.726	7.006	0.509	1.025	1.829	0.814	0.208	4.796
Δr	4.844	7.333	2.198	2.549	2.655	3.157	1.382	4.392
	S_0	S_1	S_0	S_2	S_0	S_2	S_0	S_1
ΔE	−40.678	−53.433	−54.283	−9.207	−57.831	−10.566	−27.464	56.783
BSSE	−31.214	−42.679	−39.393	7.268	−44.474	6.805	−21.727	67.791

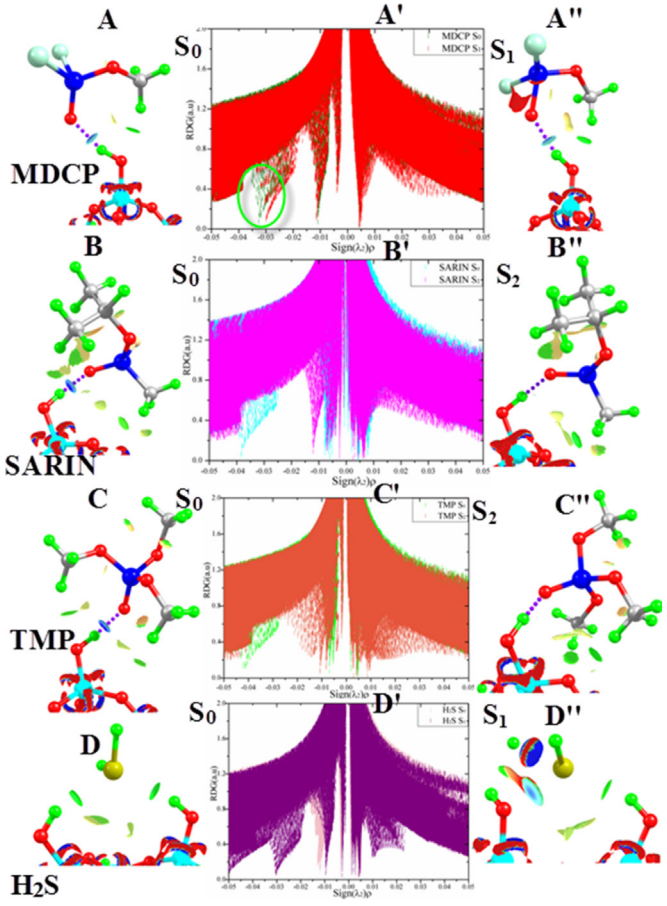

Fig. 2. Gradient isosurfaces (A, C, E, G and A′, C′, E′, G′) and the corresponding plots of the reduced density gradient (RDG) versus the electron density multiplied by the sign of the second Hessian eigenvalues (B, D, F, H and B′, D′, F′, H′).

cator of interaction strength. Large negative values of sign(λ_2)ρ are indicative of attractive interactions, such as hydrogen bonding; large positive values of sign(λ_2)ρ are indicative of nonbonding. Value of sign(λ_2)ρ near zero indicates very weak van der Waals (vdW) interaction [47,55].

In Fig. 2, the vdW interaction, hydrogen bond and steric effect of the four complexes are denoted. Blue denotes hydrogen bond interaction, yellow denotes vdW interactions and red denotes steric effect. In Fig. 2A and A', the intermolecular hydrogen bond O—H···O=P of MDCP is located at −0.035 in the ground state and right-shifts to −0.030 in the S_1 state. This shift implies its strengthening after photoexcitation. In Fig. 2B, the strong hydrogen bond interaction between O—H and O=P of SARIN is denoted as blue. This strong intermolecular hydrogen bond O—H···O=P is located at −0.040 in Fig. 2B' and disappears due to the strengthening of O—H···O=P bond. The disappearance of hydrogen bond O—H···O=P indicates that the strong hydrogen bond O—H···O=P is significantly strengthened in the S_2 state. The change of TMP system (in Fig. 2C, C′, C″) is similar to that of SARIN system. It is noted in Fig. 2D that the spike point located at −0.012 corresponds to the weak hydrogen bonds O_1—H_1···S and O_2—H_2···S, which respectively left-shifts to −0.03 and right-shift to −0.01 when excited to the S_1 state in Fig. 2D′. This change indicates that O_1—H_1···S is strengthened while O_2—H_2···S is weakened after excitation to the S_1 state. The RDG analysis is consistent with the results of geometric structure analysis and provides reliable evidence for the change of intermolecular hydrogen bond interaction.

3.4. Frontier molecular orbital analysis

Analysis of molecular orbitals (MOs) can provide insight into the nature of the excited states [59,60]. The frontier molecular orbitals (MOs) of MDCP, SARIN, TMP and H_2S and corresponding transition percent are shown in Fig. 3. It can be seen that the S_1 state of MDCP corresponds to HOMO−5 → LUMO and HOMO−6 → LUMO transition. The electron density of HOMO-5 and HOMO-6 of MDCP complex is distributed in all of the molecular system and transfers to MDCP moiety when excited to the S_1 state. This transfer implies that the S_1 state of MDCP is an intermolecular charge transfer (CT) state, which is consistent with the results of electronic excitation analysis. The electron density decrease of O=P bond in LUMO induces the weakening of intermolecular hydrogen bond interaction after the orbital transition. This result is consistent with the geometric structure analysis. For SARIN system, the electron density of HOMO and HOMO-3 is located at the silica moiety, which hardly changes in the LUMO, implying that the S_2 state of SARIN is a LE state. This change induces the electron density increase of O=P bond and thus the strengthening of intermolecular hydrogen bond interaction between P=O and H—O groups. The S_2 state of TMP corresponds to HOMO → LUMO and HOMO → LUMO + 2 transitions. The electron density change corresponding to HOMO → LUMO transition of TMP is similar to that of SARIN complex, which induces the strengthening of intermolecular hydrogen bond interaction P=O···H—O. The S_1 state of H_2S system corresponds to HOMO → LUMO transition. The electron density of HOMO transfers from silica moiety to H_2S moiety, which induces the electron density increase of S atom. The electron density of S atom causes the strengthening of O_1—H_1···S and the weakening of O_2—H_2···S with the twisting of O_2—H_2 group in the excited S_1 state.

3.5. Electron and hole analysis

In order to explain the reason for adsorption change of silica with three organophosphorous compounds and hydrogen sulfide

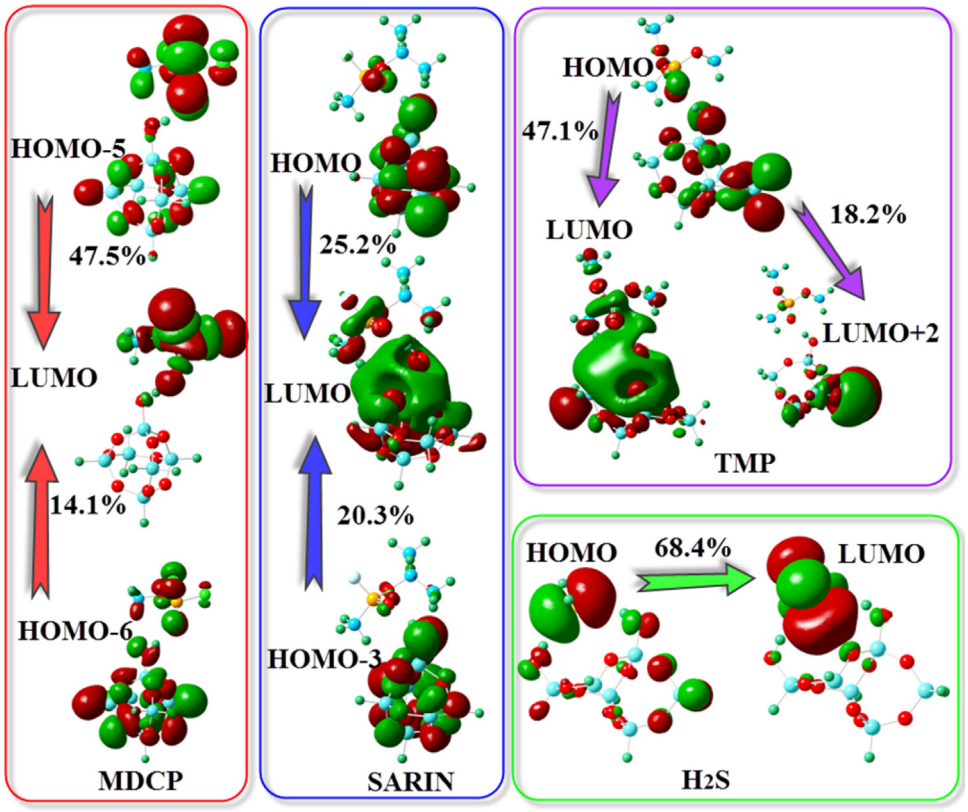

Fig. 3. The frontier molecular orbitals of MDCP, SARIN, TMP and H_2S corresponding to excited state and their transition percent.

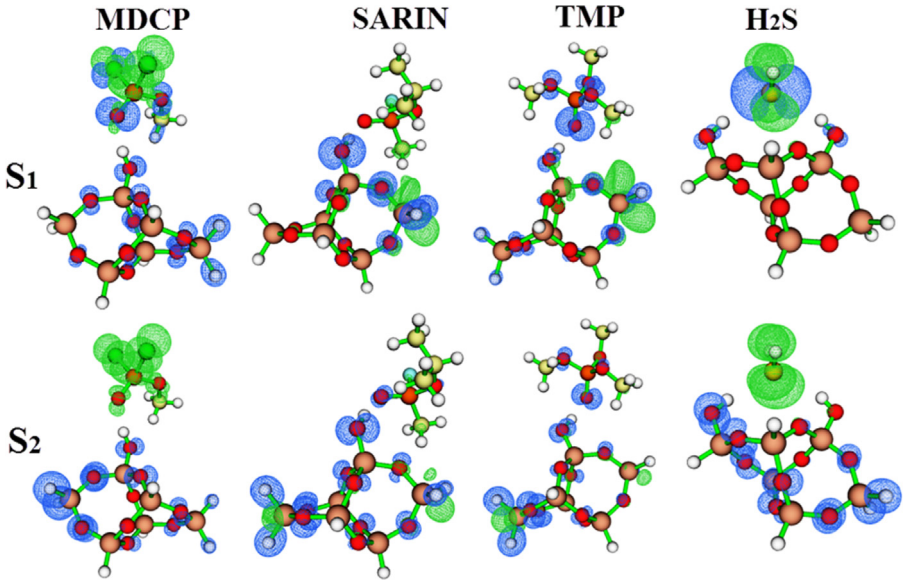

Fig. 4. The electron-hole transfer of MDCP, SARIN, TMP and H_2S in the excited S_1 and S_2 states. Green color denotes electron increase and blue color denotes electron decrease after photoexcitation. (For interpretation of the references to colour in this figure legend, the reader is referred to the web version of this article.)

after photoexcitation, the electron transfer in the excited S_1 and S_2 states of four hydrogen bonded complexes is calculated and provided in Fig. 4. The electron transfer of these four complexes after photoexcitation is analyzed by Multiwfn program [47]. Green and blue correspond to the region where electron density is respectively increased and decreased after photoexcitation. For MDCP, the electrons of O atoms in O═P and O—H groups decrease when excited to the S_1 state, which induces the weakening of hydrogen bond interaction between O═P and O—H groups. The charge transfer from silica moiety to the MDCP moiety implies that the S_1 state of MDCP is an intermolecular charge transfer (ICT) state. The electron of O═P increases significantly, implying the strengthening of O═P···O—H in the excited S_2 state. For SARIN in the excited S_2 state, the electron decrease of O—H induces the electron of H atom to be more positive compared to ground state. The charge transfer of SARIN in the S_2 state indicates that the S_2 state is a LE state. The hydrogen bond interaction between O═P and O—H will be strengthened in the S_2 state. The change of TMP is similar to that of SARIN. For

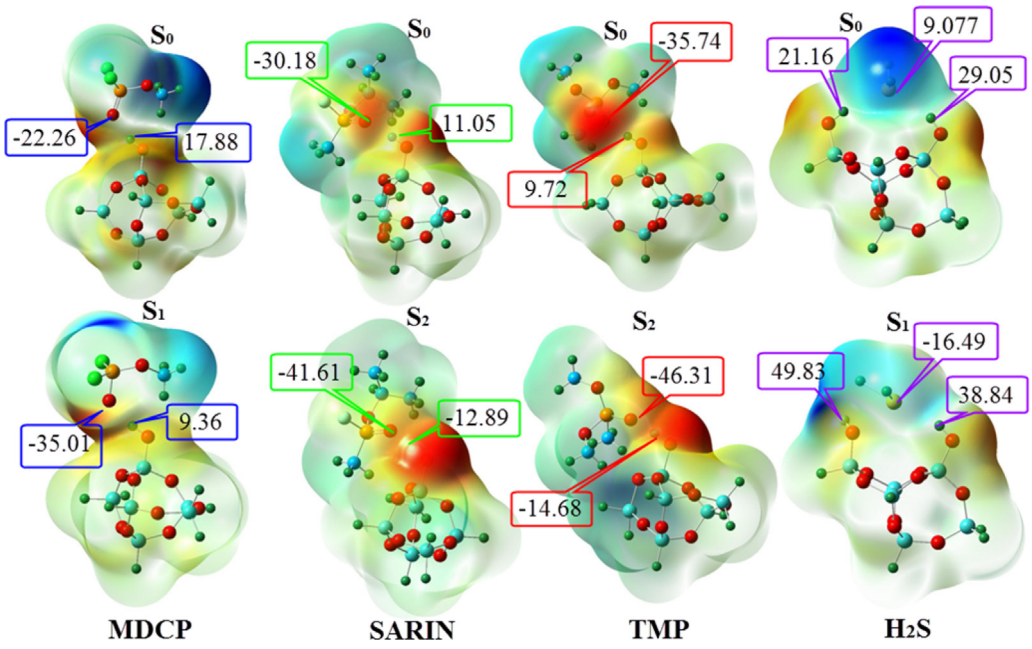

Fig. 5. The electronic potential surface and some important points of MDCP, SARIN, TMP and H_2S in ground and excited states.

H_2S system, the electrons of O atoms in two O—H groups decrease when excited to the S_1 state, while that of S atom in H_2S increases when excited to the S_1 state. This change will induce the strengthening of two intermolecular hydrogen bonds O—H···S in the S_1 state compared to that in the ground state. However, this result is not consistent with that of geometric analysis that O_1—H_1···S is strengthened while O_2—H_2···S is weakened. This difference in O_2—H_2···S between electron-hole and structure analysis is due to the twisting of O_2—H_2 group in the S_1 state.

3.6. Electrostatic potential analysis

Molecular electrostatic potential (ESP) is related to the electron density of molecular and can depict the size, shape, charge density and site of chemical reactivity of the molecules [61,62]. It is widely used in understanding the sites for electrophilic attack and nucleophilic reactions, such as intermolecular or intramolecular hydrogen bonding interactions. An electron density isosurface is mapped with electrostatic potential surface. The different color of electrostatic potential represents different value, with red representing regions of most electron negative electrostatic potential, blue representing regions of the most positive electrostatic potential, and green representing regions of zero potential.

The electrostatic potential and corresponding value of some related atoms on these four complexes' molecular surface are provided in Fig. 5. It can be seen that the red regions are located at the electronegative atoms, and that the blue regions are located at the hydrogen atoms. For MDCP, the ESP date for the O atom of O=P group changes from −22.26 kcal/mol in the ground state to −35.01 kcal/mol in the S_1 state, which may be induced by the electron transfer after excitation. The value of H atom decreases from 17.88 kcal/mol in the ground state to 9.36 kcal/mol in the S_1 state. This decrease induces the weakening of hydrogen bond interaction between O=P and O—H groups. For SARIN, the ESP value around the O atom of O=P group increases about 11.43 kcal/mol when excited to the S_2 state, and that around H atom changes from 11.05 kcal/mol to −12.89 kcal/mol. This change induces the strengthening of hydrogen bond interaction between O=P and O—H groups. The result of TMP is similar to that of SARIN. For H_2S, the ESP value around S atom is 9.07 kcal/mol in the ground state, which changes to −16.49 kcal/mol in the S_1 state. The values of H_1 and H_2 atoms increase about 9.79 kcal/mol and 28.67 kcal/mol when excited to the S_1 state. These changes of S, H_1 and H_2 atoms induce the strengthening of hydrogen bond interaction between O_1—H_1 and S atom, and the weakening for O_2—H_2···S due to the twisting of O_2—H_2 in the S_1 state. These ESP results are consistent with the analysis of molecular orbital.

3.7. Infrared spectra analysis

To delineate the changes of adsorption of MDCP, SARIN, TMP and H_2S on silica surface before and after photoexcitation, the infrared spectra of the four complexes in the ground and the excited states are calculated and provided in Fig. 6. In Fig. 6A, the peaks located at 1226 cm^{-1} and 3435 cm^{-1} correspond to P=O and O—H groups of MDCP system, which respectively red-shifts and blue-shifts to 984 cm^{-1} and 3482 cm^{-1} when excited to the S_1 state. The value of O—H group (3435 cm^{-1}) of MDCP system is consistent with experiment results (3425 cm^{-1}) [23,31]. These shifts are consistent with the bond length change of P=O and O—H groups before and after photoexcitation. The opposite change of P=O and O—H groups indicates the weakening of intermolecular hydrogen bond interaction between P=O and H—O. In Fig. 6B, peaks located at 1220 cm^{-1} and 3325 cm^{-1} correspond to P=O and O—H groups of SARIN system, which red-shift about 87 cm^{-1} and 859 cm^{-1} respectively when excited to the S_2 state. The red-shifts of P=O and O—H groups in the excited S_2 state imply the strengthening of hydrogen bond interaction between P=O and O—H. The infrared spectra change of TMP system is similar to that of SARIN system. For H_2S system in Fig. 6D, the stretching absorption peaks located at 3595 cm^{-1} and 3572 cm^{-1} correspond to the O_1—H_1 and O_2—H_2 groups respectively, red-shifting to 3509 cm^{-1} and 3548 cm^{-1} when excited to the S_1 state. This change is consistent with their bond length change before and after photoexcitation. The peaks located at 2620 cm^{-1} and 2597 cm^{-1} correspond to S-H groups of H_2S molecule. One peak disappears and the other is located at 2612 cm^{-1} when excited to the S_1 state. The red-shift of O_1—H_1 group induces the strengthening of hydrogen bond interaction between O_1—H_1 group and S atom. Nevertheless, the red-shift of O_2—H_2 group induces the weakening rather than strengthening of hydrogen bond O_2—H_2···S in the S_2

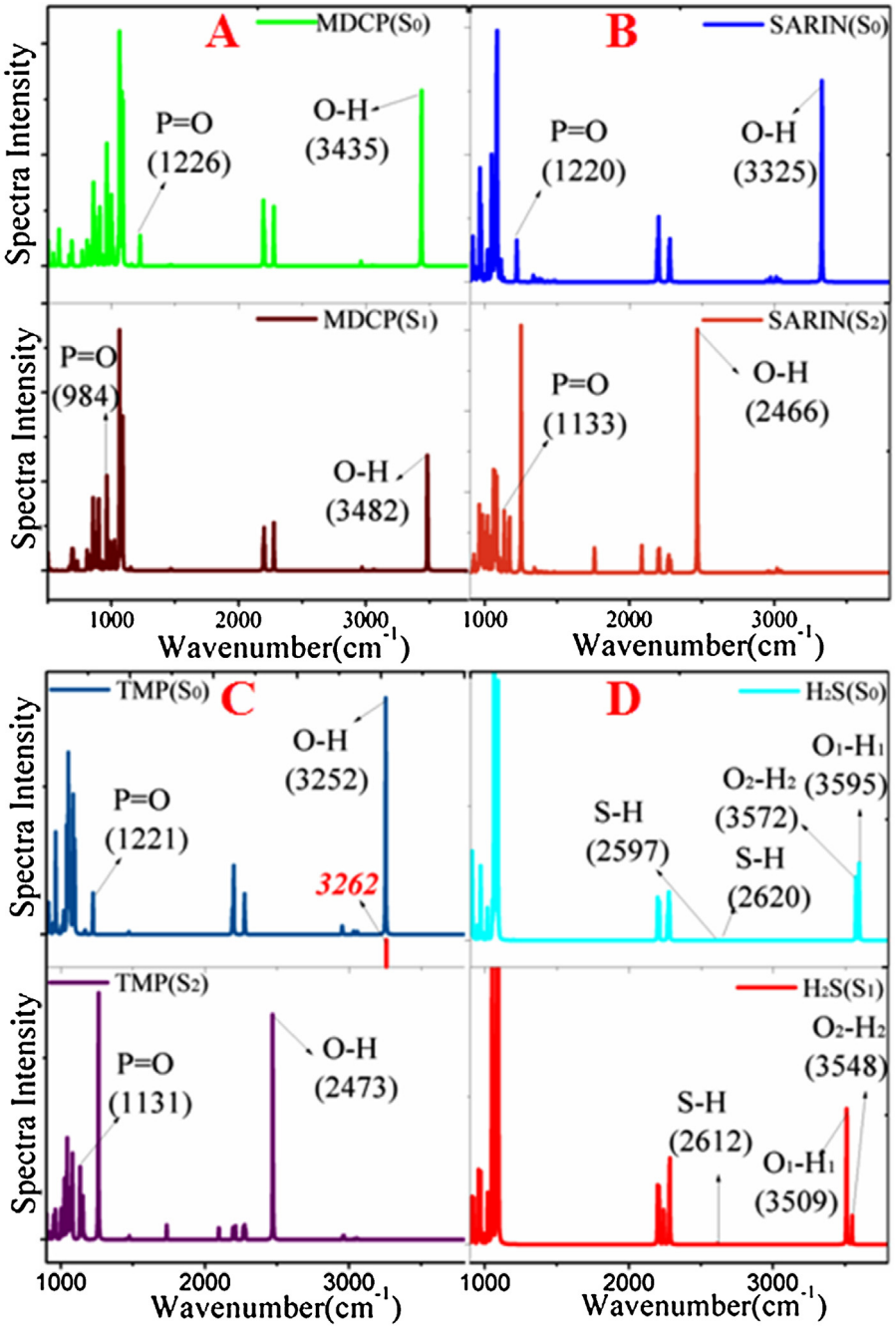

Fig. 6. The infrared spectra of MDCP, SARIN, TMP and H_2S in ground and excited states. The red line in spectra of TMP in the ground state indicates corresponding experimental result. (For interpretation of the references to colour in this figure legend, the reader is referred to the web version of this article.)

state for the twisting of O_2—H_2 group. The infrared spectra of the four complexes demonstrate the change of adsorption in excited state indirectly.

4. Conclusion

Many researchers have synthesized a large number of adsorbent and detected the environment effect on their adsorption properties, including temperature and substituent groups. The photoexcitation effect has not been seriously studied to our best knowledge. We propose a scheme for detecting adsorbent with different transition energies that: large transition energy will induce ground state adsorption; middle transition energy will induce partly ground and excited adsorption, and their ratio will change effected by environment factor; low transition energy will mainly induce higher excited state adsorption. For this purpose, the adsorption of MDCP, TMP, SARIN, and H_2S to silica surface is provided here as target sample to be theoretically studied. The adsorption energies of MDCP, SARIN and TMP in the ground state follow the trend MDCP < SARIN < TMP, which is consistent with the adsorption strengthening governed by intermolecular hydrogen bond interaction, and the desorption order of MDCP and TMP in previous related reports (*J. Phys. Chem. C*, 2013, 117, 14625). However, the adsorption energy of MDCP increases in the S_1 state, while that of SARIN and TMP decrease in the S_2 states. The intermolecular hydrogen bond of MDCP is weakened while that of SARIN and TMP is strengthened. It should be noted that the adsorption energy change of the three complexes is opposite to the change of intermolecu-

lar hydrogen bonds, implying that adsorption behaviors in excited state are remarkably different from those in the ground state and that intermolecular hydrogen bonded may not be the major factor for the adsorption. The H_2S is dissociated in the S_1 state for its adsorption energy of H_2S changes to 56.783 kJ/mol in the S_1 state from −27.464 kJ/mol in the ground state. By analyzing the frontier molecular orbital and charge transfer trends, we attribute the disagreement of adsorption energy and hydrogen bond interaction in excited state to their different charge transfer types. That is, the S_1 state of MDCP is an intermolecular charge transfer state inducing the increase of adsorption energy, while the S_2 states of SARIN and TMP are local excited states. It is concluded that hydrogen bond plays major role in the adsorption strengthen in the ground state for the adsorbent with large transition energy, and that the charge transfer types plays a major role in the S_1 state or higher state for the adsorbent with small transition energy. This work gives a reasonable interpretation of the photoexcitation effect on adsorption properties of silica and presents photoexcitation effect as an important factor for the design and detection adsorbent with different transition energy.

Acknowledgements

This work is supported by National Natural Science Foundation of China (Grant No. 11274096) and supported by Program for Innovative Research Team (in Science and Technology) in University of Henan Province (Grant No. 13IRTSTHN016). The calculation about this work was supported by The High Performance Computing Center of Henan Normal University.

References

[1] J. Quenneville, R.S. Taylor, A.C. van Duin, Reactive molecular dynamics studies of DMMP adsorption and reactivity on amorphous silica surfaces, J. Phys. Chem. C 114 (2010) 18894–18902.
[2] M. Hurley, J. Wright, G. Lushington, W. White, Quantum mechanics and mixed quantum mechanics/molecular mechanics simulations of model nerve agents with acetylcholinesterase, Theor. Chem. Acc. 109 (2003) 160–168.
[3] R.T. Delfino, T.S. Ribeiro, J.D. Figueroa-Villar, Organophosphorus compounds as chemical warfare agents: a review, J. Barz. Chem. Soc. 20 (2009) 407–428.
[4] C.N. Rusu, J.T. Yates, Adsorption and decomposition of dimethyl methylphosphonate on TiO_2, J. Phys. Chem. B 104 (2000) 12292–12298.
[5] F.R. Sidell, E.T. Takafuji, D.R. Franz, Medical Aspects of Chemical and Biological Warfare; DTIC Document, 1997.
[6] A.D.F. Toy, Phosphorus Chemistry in Everyday Living, American Chemical Society, 1976.
[7] A. Kaczmarek, L. Gorb, A.J. Sadlej, J. Leszczynski, SARIN and soman: structure and properties, Struct. Chem. 15 (2004) 517–525.
[8] W.O. Gordon, B.M. Tissue, J.R. Morris, Adsorption and decomposition of dimethyl methylphosphonate on Y2O3 nanoparticles, J. Phys. Chem. C 111 (2007) 3233–3240.
[9] A.R. Wilmsmeyer, J. Uzarski, P.J. Barrie, J.R. Morris, Interactions and binding energies of dimethyl methylphosphonate and dimethyl chlorophosphate with amorphous silica, Langmuir 28 (2012) 10962–10967.
[10] D.E. Taylor, K. Runge, M.G. Cory, D.S. Burns, J.L. Vasey, J.D. Hearn, K. Griffith, M.V. Henley, Surface binding of organophosphates on silica: comparing experiment and theory, J. Phys. Chem. C 117 (2013) 2699–2708.
[11] V.M. Bermudez, Computational study of the adsorption of trichlorophosphate dimethyl methylphosphonate, and sarin on amorphous SiO2, J. Phys. Chem. C 111 (2007) 9314–9323.
[12] A.R. Wilmsmeyer, W.O. Gordon, E.D. Davis, D. Troya, B.A. Mantooth, T.A. Lalain, J.R. Morris, Infrared spectra and binding energies of chemical warfare nerve agent simulants on the surface of amorphous silica, J. Phys. Chem. C 117 (2013) 15685–15697.
[13] C. Montauban, A. Bégos, B. Bellier, Extraction of nerve agent VX from soils, Anal. Chem. 76 (2004) 2791–2797.
[14] B. Dou, J. Li, Y. Wang, H. Wang, C. Ma, Z. Hao, Adsorption and desorption performance of benzene over hierarchically structured carbon–silica aerogel composites, J. Hazard. Mater. 196 (2011) 194–200.
[15] G.W. Wagner, R.J. O'Conno, L.R. Procell, Preliminary study on the fate of VX in concrete, Langmuir 17 (2001) 4336–4341.
[16] P.A. D'Agostino, J.R. Hancock, L.R. Provost, Determination of sarin, soman and their hydrolysis products in soil by packed capillary liquid chromatography-electrospray mass spectrometry, J. Chromatogr. A 912 (2001) 291–299.
[17] G.S. Groenewold, J.M. Williams, A.D. Appelhans, G.L. Gresham, J.E. Olson, M.T. Jeffery, B. Rowland, Hydrolysis of VX on concrete: rate of degradation by direct surface interrogation using an ion trap secondary ion mass spectrometer, Environ. Sci. Technol. 36 (2002) 4790–4794.
[18] V. Bolis, B. Fubini, L. Marchese, G. Martra, D. Costa, Hydrophilic and hydrophobic sites on dehydrated crystalline and amorphous silicas, J. Chem. Soc. Faraday Trans. 87 (1991) 497–505.
[19] I.S. Chuang, D.R. Kinney, G.E. Maciel, Interior hydroxyls of the silica gel system as studied by silicon-29 CP-MAS NMR spectroscopy, J. Am. Chem. Soc. 115 (1993) 8695–8705.
[20] D.R. Kinney, I.S. Chuang, G.E. Maciel, Water and the silica surface as studied by variable-temperature high-resolution proton NMR, J. Am. Chem. Soc. 115 (1993) 6786–6794.
[21] L. Zhuravlev, The surface chemistry of amorphous silica. Zhuravlev model, Colloid Surf. A 173 (2000) 1–38.
[22] A. Rimola, D. Costa, M. Sodupe, J.-F. Lambert, P. Ugliengo, Silica surface features and their role in the adsorption of biomolecules: computational modeling and experiments, Chem. Rev. 113 (2013) 4216–4313.
[23] S.M. Kanan, C.P. Tripp, An infrared study of adsorbed organophosphonates on silica: a prefiltering strategy for the detection of nerve agents on metal oxide sensors, Langmuir 17 (2001) 2213–2218.
[24] V. Bermudez, Effect of humidity on the interaction of dimethyl methylphosphonate (DMMP) vapor with SiO2 and Al2O3 surfaces, studied using infrared attenuated total reflection spectroscopy, Langmuir 26 (2010) 18144–18154.
[25] M. Henderson, T. Jin, J. White, A TPD/AES study of the interaction of dimethyl methylphosphonate with iron oxide (.alpha.-Fe2O3) and silicon dioxide, J. Phys. Chem. C 90 (1986) 4607–4611.
[26] L. Zhuravlev, Concentration of hydroxyl groups on the surface of amorphous silicas, Langmuir 3 (1987) 316–318.
[27] Y.C. Yang, J.A. Baker, J.R. Ward, Decontamination of chemical warfare agents, Chem. Rev. 92 (1992) 1729–1743.
[28] D. Troya, A.C. Edwards, J.R. Morris, Theoretical study of the adsorption of organophosphorous compounds to models of a silica surface, J. Phys. Chem. C 117 (2013) 14625–14634.
[29] M.L. Hair, W. Hertl, Adsorption on hydroxylated silica surfaces, J. Phys. Chem. 73 (1969) 4269–4276.
[30] K. Kim, O.G. Tsay, D.A. Atwood, D.G. Churchill, Destruction and detection of chemical warfare agents, Chem. Rev. 111 (2011) 5345–5403.
[31] S.M. Kanan, C.P. Tripp, Prefiltering strategies for metal oxide based sensors: the use of chemical displacers to selectively dislodge adsorbed organophosphonates from silica surfaces, Langmuir 18 (2002) 722–728.
[32] H. Tsubomura, Nature of the hydrogen bond. III. the measurement of the infrared absorption intensities of free and hydrogen-bonded OH bands. theory of the increase of the intensity due to the hydrogen bond, J. Chem. Phys. 24 (1956) 927–931.
[33] J.S. Rieck, A.T. Bell, Influence of adsorption and mass transfer effects on temperature-programmed desorption from porous catalysts, J. Catal. 85 (1984) 143–153.
[34] A.L.H. Chung, M.J.S. Dewar, Ground states of conjugated molecules. I. Semiempirical SCF MO treatment and its application to aromatic hydrocarbons, J. Chem. Phys. 42 (1965) 756–766.
[35] S. Sunakawa, S. Yamasaki, T. Kebukawa, Energy spectrum of the excitations in liquid HeHum II, Prog. Theor. Phys. 41 (1969) 919–940.
[36] W.J. Hehre, A Guide to Molecular Mechanics and Quantum Chemical Calculations[M], Wavefunction, Irvine, CA, 2003.
[37] A. Dreuw, M. Head-Gordon, Single-reference ab initio methods for the calculation of excited states of large molecules, Chem. Rev. 105 (2005) 4009–4037.
[38] J. Abelard, A.R. Wilmsmeyer, A.C. Edwards, W.O. Gordon, E.M. Durke, C.J. Karwacki, D. Troya, J.R. Morris, Adsorption of 2-chloroethyl ethyl sulfide on silica: binding mechanism and energy of a bifunctional hydrogen-bond acceptor at the gas–surface interface, J. Phys. Chem. C 119 (2014) 365–372.
[39] E.D. Davis, W.O. Gordon, A.R. Wilmsmeyer, D. Troya, J.R. Morris, Chemical warfare agent surface adsorption: hydrogen bonding of sarin and soman to amorphous silica, J. Phys. Chem. Lett. 5 (2014) 1393–1399.
[40] S.L. Warring, D.A. Beattie, A.J. McQuillan, Surficial siloxane-to-silanol interconversion during room-temperature hydration/dehydration of amorphous silica films observed by ATR-IR and TIR-Raman spectroscopy, Langmuir 32 (2016) 1568–1576.
[41] N. Wang, J. Park, T.G. Ellis, The mechanism of hydrogen sulfide adsorption on fine rubber particle media (FRPM), J. Hazard. Mater. 260 (2013) 921–928.
[42] S.H. Esmaeili Faraj, M. Nasr Esfahany, M. Jafari-Asl, N. Etesami, Hydrogen sulfide bubble absorption enhancement in water-based nanofluids, Ind. Eng. Chem. Res. 53 (2014) 16851–16858.
[43] O. Mabayoje, M. Seredych, T.J. Bandosz, Enhanced reactive adsorption of hydrogen sulfide on the composites of graphene/graphite oxide with copper (Hydr)oxychlorides, ACS Appl. Mater. Interfaces 4 (2012) 3316–3324.
[44] M.J. Frisch, G.W. Trucks, H.B. Schlegel, G.E. Scuseria, M.A. Robb, J.R. Cheeseman, G. Scalmani, V. Barone, B. Mennucci, G.A. Petersson, H. Nakatsuji, M. Caricato, X. Li, H.P. Hratchian, A.F. Izmaylov, J. Bloino, G. Zheng, J.L. Sonnenberg, M. Hada, M. Ehara, K. Toyota, R. Fukuda, J. Hasegawa, M. Ishida, T. Nakajima, Y. Honda, O. Kitao, H. Nakai, T. Vreven, J.A. Montgomery, Jr., J.E. Peralta, F. Ogliaro, M. Bearpark, J.J. Heyd, E. Brothers, K.N. Kudin, V.N. Staroverov, T. Keith, R. Kobayashi, J. Normand, K. Raghavachari, A. Rendell, J.C. Burant, S.S. Iyengar, J. Tomasi, M. Cossi, N. Rega, J.M. Millam, M. Klene, J.E.

Knox, J.B. Cross, V. Bakken, C. Adamo, J. Jaramillo, R. Gomperts, R.E. Stratmann, O. Yazyev, A.J. Austin, R. Cammi, C. Pomelli, J.W. Ochterski, R.L. Martin, K. Morokuma, V.G. Zakrzewski, G.A. Voth, P. Salvador, J.J. Dannenberg, S. Dapprich, A.D. Daniels, O. Farkas, J.B. Foresman, J.V. Ortiz, J. Cioslowski, D.J. Fox, Gaussian, Inc., Wallingford CT, 2010.

[45] A.D. Becke, Density-functional thermochemistry. III. The role of exact exchange, J. Chem. Phys. 98 (1993) 5648–5652.

[46] C. Lee, W. Yang, R.G. Parr, Development of the Colle-Salvetti correlation-energy formula into a functional of the electron density, Phys. Rev. B 37 (1988) 785.

[47] T. Lu, F. Chen, Multiwfn: a multifunctional wavefunction analyzer, J. Comput. Chem. 33 (2012) 580–592.

[48] C. Li, C. Ma, D. Li, Y. Liu, Excited state intramolecular proton transfer (ESIPT) of 6-amino-2-(2′-hydroxyphenyl) benzoxazole in dichloromethane and methanol: a TD-DFT quantum chemical study, J. Lumin. 172 (2016) 29–33.

[49] Y. Yang, Y. Liu, D. Yang, H. Li, K. Jiang, J. Sun, Theoretical study on the dehydrogenation reaction of dihydrogen bonded phenol–borane-trimethylamine in the excited state, Phys. Chem. Chem. Phys. 17 (2015) 32132–32139.

[50] H. Li, Y. Liu, Y. Yang, D. Yang, J. Sun, Influences of hydrogen bonding dynamics on adsorption of ethyl mercaptan onto functionalized activated carbons: a DFT/TDDFT study, J. Photochem. Photobiol. A 291 (2014) 9–15.

[51] Y. Liu, Y. Yang, K. Jiang, D. Shi, J. Sun, Excited-state N-H···S hydrogen bond between indole and dimethyl sulfide: time-dependent density functional theory study, Phys. Chem. Chem. Phys. 13 (2011) 15299–15304.

[52] G.-J. Zhao, K.-L. Han, Hydrogen bonding in the electronic excited state, Acc. Chem. Res. 45 (2011) 404–413.

[53] G.-J. Zhao, K.-L. Han, Site-specific solvation of the photoexcited protochlorophyllide a in methanol: formation of the hydrogen-bonded intermediate state induced by hydrogen-bond strengthening, Biophys. J. 94 (2008) 38–46.

[54] F.P. Gasparro, M. Mitchnick, J.F. Nash, A review of sunscreen safety and efficacy, Photochem. Photobiol. 68 (1998) 243–256.

[55] M.M. Caldwell, A.H. Teramura, M. Tevini, The changing solar ultraviolet climate and the ecological consequences for higher plants, Trends Ecol. Evol. 4 (1989) 363–367.

[56] S. Jantaro, W. Baebprasert, C. Piyamawadee, O. Sodsuay, A. Incharoensakdi, Exogenous spermidine alleviates UV-induced growth inhibition of Synechocystis sp. PCC 6803 via reduction of hydrogen peroxide and malonaldehyde levels, Appl. Biochem. Biotechnol. 173 (2014) 1145–1156.

[57] C.A. Guido, P. Cortona, B. Mennucci, C. Adamo, On the metric of charge transfer molecular excitations: a simple chemical descriptor, J. Chem. Theory Comput. 9 (2013) 3118–3126.

[58] E.R. Johnson, S. Keinan, P. Mori-Sanchez, J. Contreras-Garcia, A.J. Cohen, W. Yang, Revealing noncovalent interactions, J. Am. Chem. Soc. 132 (2010) 6498–6506.

[59] V. Lemaur, M. Steel, D. Beljonne, J.-L. Brédas, J. Cornil, Photoinduced charge generation and recombination dynamics in model donor/acceptor pairs for organic solar cell applications: a full quantum-chemical treatment, J. Am. Chem. Soc. 127 (2005) 6077–6086.

[60] X. Fua, Q. Zhou, Y. Ding, P. Song, F. Ma, External electric field dependent photoinduced charge transfer in Donor-PC71BM system for an organic solar cell, J. At. Mol. Sci. 7 (2016) 64–76.

[61] B. Galabov, P. Bobadova-Parvanova, Molecular electrostatic potential as reactivity index in hydrogen bonding: ab initio molecular orbital study of complexes of nitrile and carbonyl compounds with hydrogen fluoride, J. Phys. Chem. A 103 (1999) 6793–6799.

[62] P.W. Kenny, Hydrogen bonding electrostatic potential, and molecular design, J. Chem. Inf. Model. 49 (2009) 1234–1244.